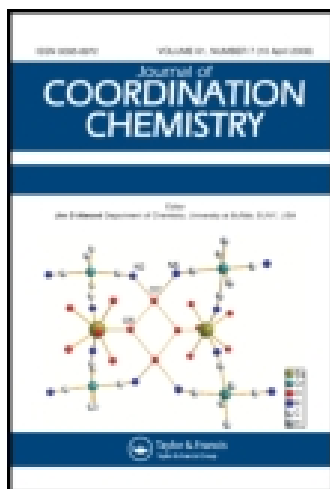


This article was downloaded by: [FU Berlin]

On: 12 November 2014, At: 03:30

Publisher: Taylor & Francis

Informa Ltd Registered in England and Wales Registered Number: 1072954 Registered office: Mortimer House, 37-41 Mortimer Street, London W1T 3JH, UK



Journal of Coordination Chemistry

Publication details, including instructions for authors and subscription information:

<http://www.tandfonline.com/loi/gcoo20>

Molecular structure and electrochemistry of carbon-bridged diferrocenyl compounds

Rui-Jun Xie^a, Li-Min Han^a, Quan-Ling Suo^a, Hai-Long Hong^a & Mei-Hua Luo^a

^a Chemical Engineering College, Inner Mongolia University of Technology, Hohhot 010051, P.R. China

Published online: 11 Jun 2010.

To cite this article: Rui-Jun Xie, Li-Min Han, Quan-Ling Suo, Hai-Long Hong & Mei-Hua Luo (2010) Molecular structure and electrochemistry of carbon-bridged diferrocenyl compounds, *Journal of Coordination Chemistry*, 63:10, 1700-1710, DOI: [10.1080/00958972.2010.487102](https://doi.org/10.1080/00958972.2010.487102)

To link to this article: <http://dx.doi.org/10.1080/00958972.2010.487102>

PLEASE SCROLL DOWN FOR ARTICLE

Taylor & Francis makes every effort to ensure the accuracy of all the information (the "Content") contained in the publications on our platform. However, Taylor & Francis, our agents, and our licensors make no representations or warranties whatsoever as to the accuracy, completeness, or suitability for any purpose of the Content. Any opinions and views expressed in this publication are the opinions and views of the authors, and are not the views of or endorsed by Taylor & Francis. The accuracy of the Content should not be relied upon and should be independently verified with primary sources of information. Taylor and Francis shall not be liable for any losses, actions, claims, proceedings, demands, costs, expenses, damages, and other liabilities whatsoever or howsoever caused arising directly or indirectly in connection with, in relation to or arising out of the use of the Content.

This article may be used for research, teaching, and private study purposes. Any substantial or systematic reproduction, redistribution, reselling, loan, sub-licensing, systematic supply, or distribution in any form to anyone is expressly forbidden. Terms & Conditions of access and use can be found at <http://www.tandfonline.com/page/terms-and-conditions>

Molecular structure and electrochemistry of carbon-bridged diferrocenyl compounds

RUI-JUN XIE, LI-MIN HAN*, QUAN-LING SUO, HAI-LONG HONG
and MEI-HUA LUO

Chemical Engineering College, Inner Mongolia University of Technology,
Hohhot 010051, P.R. China

(Received 23 June 2010; in final form 2 March 2010)

Four diferrocenyl compounds: $\text{FcC}(\text{CH}_3)_2\text{Fc}$ (**1**), $\text{Fc}(\text{CH}_3)\text{C}(\text{C}_2\text{H}_5)\text{Fc}$ (**2**), $\text{Fc}(\text{CH}_3)\text{C}(\text{C}_3\text{H}_7)\text{Fc}$ (**3**), and $\text{Fc}(\text{CH}_3)\text{C}(\text{C}_6\text{H}_5)\text{Fc}$ (**4**) were synthesized and characterized by NMR, FT-IR, MS, and elemental analysis. The molecular structures were determined by using X-ray single crystal diffraction. The electrochemical interactions between two ferrocenyl units in these compounds were investigated by cyclic voltammetry and theoretical calculation. The electron density of bridging carbon was a key factor for the separation of two ferrocenyl units.

Keywords: Diferrocene; Electrochemical interaction; Carbon-bridge; Substituent

1. Introduction

During the past three decades, various atom-bridged diferrocenyl derivatives [1–5], such as the “C” [6], “Si” [7], “P” [8], chalcogen (S, Se, and Te) [9], and Hg- [10] bridged diferrocenes, have been prepared due to their potential applications in magnetic, electronic, and optical devices. Interest was concentrated not only on how to construct these atom-bridged diferrocene systems, but also on the electrochemical interaction of two ferrocenyl units. Generally, the redox potential separation value, ΔE , between ferrocenyl units provides a direct measure of electrochemical interaction, and ΔE values are under the influence of the bridged atom [11], the bridge type [12–15], the distance of redox units [16], and molecular topology [17].

In atom-bridged diferrocenes, there are only two possible interaction types, as previously stated by Watts [6], between two ferrocenyl units: (a) interaction propagates through the bridge or (b) direct Fe–Fe space effect. Yuan *et al.* [18] deduced that the Fe–Fe distance was the key factor for the interaction of two ferrocenyl units in “C”-bridged diferrocenyl derivatives, but no single crystal data supported their conclusions.

In order to understand the key factor for electrochemical interactions between two ferrocenyl units in “C”-bridged diferrocenyl derivatives, four diferrocenyl compounds

*Corresponding author. Email: hanlimin_442@hotmail.com

were prepared in this work. Electrochemical interactions between two ferrocenyl units were investigated by molecular structure analysis, cyclic voltammetry, and calculations.

2. Experimental

2.1. General procedures

All manipulations were performed in a pure argon atmosphere. Solvents were purified, dried, and distilled under argon prior to use. Reactions were monitored by TLC. Column chromatographic separations and purification were performed on 200–300 mesh neutral alumina. All other chemicals were purchased from Alfa Aesar Chem.

IR spectra were recorded on a Nicolet FT-IR spectrometer in KBr discs. Elemental analyses were carried out on an Elementar var III-type analyzer. ^1H and ^{13}C NMR spectra in CDCl_3 were recorded on a Bruker-500 MHz spectrometer. Mass spectra were determined using a Micromass LCT instrument and melting points were determined using an XT-4 melting point apparatus. The platinum disk of radius 0.8 mm was used as working electrode for cyclic voltammetry. The electrode surface was polished with 0.05 μm alumina before each run. The auxiliary electrode was a coiled platinum wire. The reference electrode was a $\text{Ag}|\text{AgCl}$ electrode. The supporting electrolyte used in all electrochemical experiments was tetra-*n*-butylammonium hexafluorophosphate (TBAHFP) at 0.5 M. The potentiostat was CHI-760C. We employed argon as purge gas to eliminate oxygen from the one-compartment cell before the electrochemical experiments. Single crystal structures were obtained by a Bruker SMART APEX CCD diffractometer with graphite monochromated $\text{Mo-K}\alpha$ ($\lambda = 0.71073 \text{ \AA}$) radiation. All data were collected at 113(2) K using the φ - and ω -scan techniques. Suitable crystals of **1–4** (with volume of 0.26 mm \times 0.21 mm \times 0.04 mm, 0.22 mm \times 0.20 mm \times 0.08 mm, 0.22 mm \times 0.18 mm \times 0.14 mm, and 0.20 mm \times 0.16 mm \times 0.12 mm) were selected. The structure solution and refinement were performed by SHELXSL97 [19].

2.2. Synthesis of $\text{FcC}(\text{CH}_3)_2\text{Fc}$ (**1**), $\text{Fc}(\text{CH}_3)\text{C}(\text{C}_2\text{H}_5)\text{Fc}$ (**2**), $\text{Fc}(\text{CH}_3)\text{C}(\text{C}_3\text{H}_7)\text{Fc}$ (**3**), and $\text{Fc}(\text{CH}_3)\text{C}(\text{C}_6\text{H}_5)\text{Fc}$ (**4**)

Toluene (30 mL), methanol (7 mL), sulfuric acid (3.5 mL), and ferrocene (5.6 g, 0.03 mol) were added into a three-neck flask under an atmosphere of pure argon. Then acetone (3.3 mL, 0.045 mol) was added dropwise at 80°C. After the solution was stirred for 6 h at 80°C, then cooled to room temperature, the reaction mixture was extracted with toluene, the organic phase was washed by Na_2CO_3 aqueous solution and distilled water, and desiccated by anhydrous MgSO_4 . The solvent was removed *in vacuo*, and the residues were subjected to chromatographic separation on a neutral alumina column (Φ 2 cm \times 35 cm). Elution with a mixture of hexane:dichloromethane (10:1, v/v) afforded a yellow band for **1**. Yield: 54.37%. m.p. 128–129°C. Anal Calcd for $\text{C}_{23}\text{H}_{24}\text{Fe}_2$: C, 67.03; H, 5.87. Found: C, 66.89; H, 6.14. IR(KBr disk): 3089.30 [Cp , $\nu_{\text{C-H}}$](Cp = cyclopentadiene); 2980.32, 2929.73, 2855.78 [$\text{C}(\text{CH}_3)_2$, $\nu_{\text{C-H}}$]; 1100.54, 999.35 [Cp , $\gamma_{\text{C-H}}$]; 816.43 [Cp , $\delta_{\text{C-H}}$]. $^1\text{H-NMR}$ (CDCl_3 , δ): 4.160, 4.100, 4.034 [Fc, 18H]; 1.567, 1.534, 1.504 [$\text{C}(\text{CH}_3)_2$, 6H]. $^{13}\text{C-NMR}$ (CDCl_3 , δ): 66.06–77.42 [Cp , 20C], 30.60 [$\text{CH}_3(\text{C})\text{CH}_3$, 2C], 33.36 [$(\text{CH}_3)_2\text{C}$, 1C]. MS (ESI, relative

abundance): 412(M^+ , 100%). The single crystal of **1** was obtained by re-crystallizing from hexane:dichloromethane (4:1, v/v) at room temperature.

Similar to the above processes, acetone was replaced by butanone (4 mL, 0.045 mol), 2-pentanone (4.8 mL, 0.045 mol) and acetophenone (7 mL, 0.06 mol) to obtain $\text{Fc}(\text{CH}_3)\text{C}(\text{C}_2\text{H}_5)\text{Fc}$ (**2**), $\text{Fc}(\text{CH}_3)\text{C}(\text{C}_3\text{H}_7)\text{Fc}$ (**3**), and $\text{Fc}(\text{CH}_3)\text{C}(\text{C}_6\text{H}_5)\text{Fc}$ (**4**), respectively.

Compound **2**: Yield: 62.43%. m.p. 99–100°C. Anal Calcd for $\text{C}_{24}\text{H}_{26}\text{Fe}_2$: C, 67.64; H, 6.15. Found: C, 67.31; H, 6.19. IR (KBr disk): 3093.19 [Cp , $\nu_{\text{C-H}}$]; 2972.54, 2929.73, 2879.14 [CCH_3 , CCH_2CH_3 , $\nu_{\text{C-H}}$]; 1108.32, 995.48 [Cp , $\gamma_{\text{C-H}}$]; 812.54 [Cp , $\delta_{\text{C-H}}$]. $^1\text{H-NMR}$ (CDCl_3 , δ): 4.156, 4.010 [Fc , 18H]; 1.943, 1.920, 1.895, 1.873 [$\text{CCH}_2(\text{CH}_3)$, 2H]; 1.510, 1.461 [(CCH_2) CH_3 , 3H]; 0.919, 0.897, 0.874 [CCH_3 , 3H]. $^{13}\text{C-NMR}$ (CDCl_3 , δ): 66.06–77.41 [Cp , 20C], 9.47 [(CCH_2) CH_3 , 1C], 23.80 [$\text{CH}_3(\text{CCH}_2\text{CH}_3)$, 1C], 33.34 [(CH_3) $\text{CH}_2(\text{CH}_3)$, 1C], 36.55 [(CH_3) $\text{C}(\text{CH}_2\text{CH}_3)$, 1C]. MS (ESI, relative abundance): 426(M^+ , 100%).

Compound **3**: Yield: 63.15%. m.p. 106–107°C. Anal Calcd for $\text{C}_{25}\text{H}_{28}\text{Fe}_2$: C, 68.21; H, 6.41. Found: C, 67.99; H, 6.52. IR (KBr disk): 3093.19 [Cp , $\nu_{\text{C-H}}$]; 2956.97, 2929.73, 2867.46 [CCH_3 , $\text{CCH}_2\text{CH}_2\text{CH}_3$, $\nu_{\text{C-H}}$]; 1104.43, 999.35 [Cp , $\gamma_{\text{C-H}}$]; 816.43 [Cp , $\delta_{\text{C-H}}$]. $^1\text{H-NMR}$ (CDCl_3 , δ): 4.075, 3.973 [Fc , 18H]; 1.827, 1.811, 1.800, 1.785, 1.771 [(CCH_2CH_2) CH_3 , 3H]; 1.596 [CCH_3 , 3H]; 1.247, 1.221, 1.194, 1.168 [(CCH_2) $\text{CH}_2(\text{CH}_3)$, 2H]; 0.879, 0.856, 0.831 [$\text{CCH}_2(\text{C}_2\text{H}_5)$, 2H]. $^{13}\text{C-NMR}$ (CDCl_3 , δ): 66.51–77.41 [Cp , 20C], 15.03 [(CCH_2CH_2) CH_3 , 1C], 18.11 [(CCH_2) $\text{CH}_2(\text{CH}_3)$, 1C], 24.73 [$\text{CH}_3(\text{CCH}_2\text{CH}_2\text{CH}_3)$, 1C], 36.46 [(CH_3) $\text{C}(\text{CH}_2\text{CH}_2\text{CH}_3)$, 1C], 41.9 [(CH_3) $\text{CH}_2(\text{CH}_2\text{CH}_3)$, 1C]. MS (ESI, relative abundance): 440(M^+ , 100%).

Compound **4**: Yield: 21.36%. m.p. 210–211°C. Anal Calcd for $\text{C}_{28}\text{H}_{26}\text{Fe}_2$: C, 70.92; H, 5.53. Found: C, 70.69; H, 5.57. IR (KBr disk): 3089.30 [Cp , Ph , $\nu_{\text{C-H}}$]; 2984.22, 2933.62, 2867.46 [CCH_3 , $\nu_{\text{C-H}}$]; 1100.54, 995.46 [Cp , $\gamma_{\text{C-H}}$]; 816.43 [Cp , $\delta_{\text{C-H}}$]. $^1\text{H-NMR}$ (CDCl_3 , δ): 4.075–3.973 [Fc , 18H]; 1.45–1.49 [(C) CH_3 , 3H]; 7.29–7.40 [Ph , 5H]. $^{13}\text{C-NMR}$ (CDCl_3 , δ): 66.53–77.41 [Cp , 20C], 126.85–148.56 [Ph , 6C], 28.39 [(C) CH_3 , 1C], 41.36 [(C) CH_3 , 1C]. MS (ESI, relative abundance): 474 (M^+ , 100%).

Single crystals of **2–4** were obtained by re-crystallizing from hexane:dichloromethane (4:1, v/v) at room temperature.

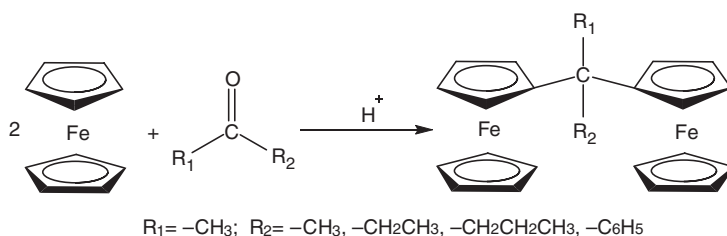
3. Results and discussion

3.1. Reactions and characterization of 1–4

The reactions carried out in this work are illustrated with scheme 1. Compounds **1–4** were prepared by the acid-catalyzed condensation of ferrocene and corresponding ketone. The four compounds were confirmed by FT-IR, $^1\text{H-NMR}$, $^{13}\text{C-NMR}$, elemental analysis, and MS.

3.2. Molecular structures of 1–4

The molecular structures of **1–4** were determined by X-ray single crystal diffraction. Crystal data and relevant structural parameters are enumerated in table 1.



Scheme 1. The reactions carried out for the synthesis of 1–4.

Table 1. Crystal data and relevant structural parameters of 1–4.

Identification code	1	2	3	4
Empirical formula	C ₂₃ H ₂₄ Fe ₂	C ₂₄ H ₂₆ Fe ₂	C ₂₅ H ₂₇ Fe ₂	C ₂₈ H ₂₆ Fe ₂
Formula weight	412.12	426.15	439.17	474.19
Temperature (K)	113(2)	113(2)	113(2)	113(2)
Wavelength (Å)	0.71073	0.71073	0.71073	0.71073
Crystal system	Tetragonal	Monoclinic	Monoclinic	Triclinic
Space group	<i>P41212</i>	<i>P2(1)/c</i>	<i>P2(1)/n</i>	<i>P-1</i>
Unit cell dimensions (Å, °)				
<i>a</i>	8.2299(12)	9.4852(19)	9.5968(19)	8.3610(17)
<i>b</i>	8.2299(12)	13.505(3)	10.648(2)	10.670(2)
<i>c</i>	52.943(11)	15.048(3)	19.533(4)	12.450(3)
α	90	90	90	76.34(3)
β	90	102.75(3)	101.08(3)	78.70(3)
γ	90	90	90	75.13(3)
Volume (Å ³), <i>Z</i>	3585.9(10), 8	1880.1(7), 4	1958.7(7), 4	1032.3(4), 2
Calculated density (calculated) (mg m ⁻³)	1.527	1.506	1.489	1.526
Absorption coefficient (mm ⁻¹)	1.620	1.547	1.488	1.418
<i>F</i> (000)	1712	888	916	492
Crystal size (mm ³)	0.20 × 0.18 × 0.12	0.22 × 0.20 × 0.08	0.22 × 0.18 × 0.14	0.20 × 0.16 × 0.12
θ range for data collection (°)	2.50–25.02°	2.05–25.02°	2.12–25.02°	1.70–25.02°
Limiting indices	–9 ≤ <i>h</i> ≤ 9; –9 ≤ <i>k</i> ≤ 9; –50 ≤ <i>l</i> ≤ 63	–11 ≤ <i>h</i> ≤ 11; –10 ≤ <i>k</i> ≤ 16; –17 ≤ <i>l</i> ≤ 17	–11 ≤ <i>h</i> ≤ 11; –12 ≤ <i>k</i> ≤ 11; –19 ≤ <i>l</i> ≤ 23	–9 ≤ <i>h</i> ≤ 9; –12 ≤ <i>k</i> ≤ 11; –14 ≤ <i>l</i> ≤ 14
Reflections collected	9697	12,430	12,786	7458
Independent reflections	2931	3306	3442	3586
Completeness to θ (%)	93.4	99.7	99.4	98.7
Max. and min. transmission	0.8294/0.7377	0.8862/0.7271	0.8188/0.7355	0.8483/0.7646
Data/restraints/parameters	2940/138/228	3306/0/235	3442/0/244	3586/0/271
Goodness-of-fit on <i>F</i> ²	1.039	0.561	1.147	1.117
Final <i>R</i> indices [<i>I</i> > 2 σ (<i>I</i>)]	<i>R</i> ₁ = 0.0653; <i>wR</i> ₂ = 0.1154	<i>R</i> ₁ = 0.0261; <i>wR</i> ₂ = 0.0708	<i>R</i> ₁ = 0.0282; <i>wR</i> ₂ = 0.0809	<i>R</i> ₁ = 0.0325; <i>wR</i> ₂ = 0.0909
<i>R</i> indices (all data)	<i>R</i> ₁ = 0.0812; <i>wR</i> ₂ = 0.1196	<i>R</i> ₁ = 0.0304; <i>wR</i> ₂ = 0.0749	<i>R</i> ₁ = 0.0312; <i>wR</i> ₂ = 0.0824	<i>R</i> ₁ = 0.0381; <i>wR</i> ₂ = 0.1096
Largest difference peak and hole (e Å ⁻³)	–0.414 and –0.586	0.295 and –0.394	0.853 and –0.712	0.485 and –0.567

The molecular structures are shown in figures 1–4; selected bond lengths and angles are listed in tables 2 and 3.

Bond angles around the bridge carbons range from 106.5° to 111.60°, which is in accord with sp³ hybridization. The average length of C–C bonds in Fc units is 1.42 Å

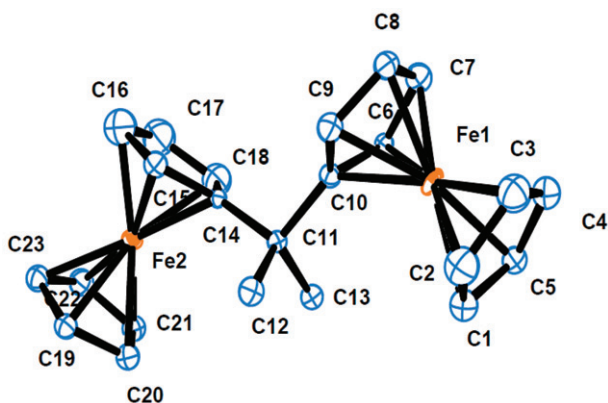


Figure 1. The molecular structure of 1.

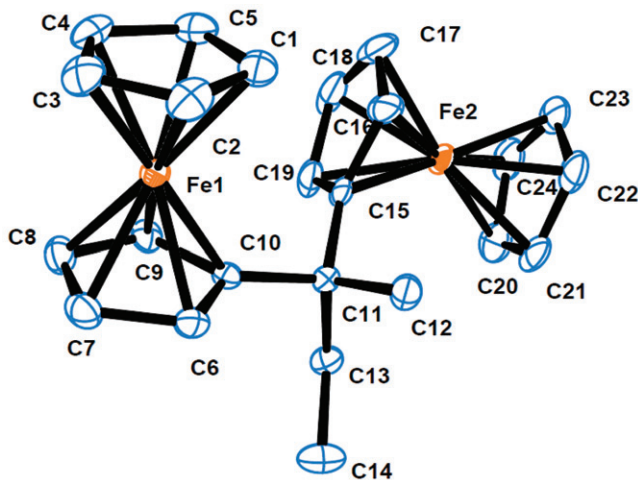


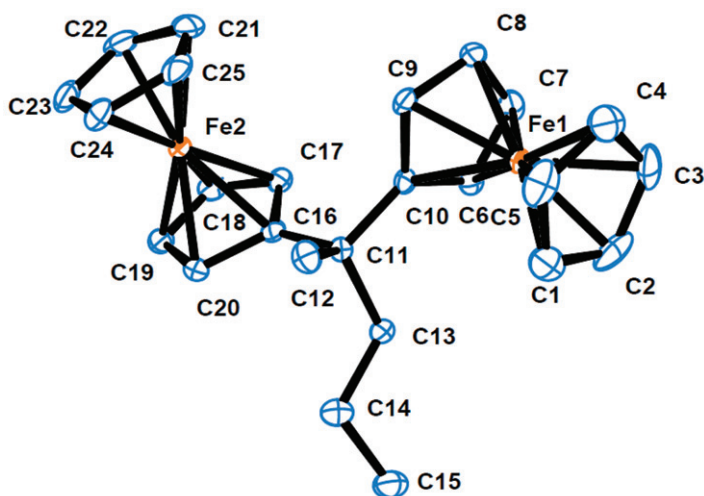
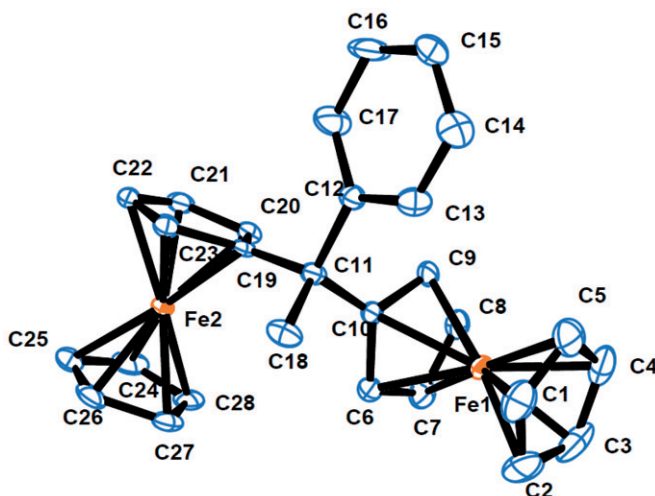
Figure 2. The molecular structure of 2.

while the average length of Fe–C bonds is 2.04 Å. The mean length from Fe to Cp ring plane is 1.65 Å. The mean dihedral angle of two Cp ring planes in each ferrocene is 3.5°, indicating the parallel Cp rings in 1–4.

3.3. Electrochemistry

The cyclic voltammograms (CV) of 1–4 are depicted in figure 5. All curves display two electrochemically reversible redox waves and each step is one-electron transfer, assigned to the two Fe_(II)/Fe_(III) redox couples. The oxidation potential difference (ΔE) between $E_{a,1}$ and $E_{a,2}$ of the ferrocenyl units are 200, 220, 223, and 195 mV, respectively, indicating the substituent on carbon influences potential difference.

According to Watts and Yuan [2, 18], the Fe–Fe distance should be key for potential separation. However, if direct Fe–Fe distance is the key factor for ΔE , the ΔE shall

Figure 3. The molecular structure of **3**.Figure 4. The molecular structure of **4**.

increase with the decreasing Fe–Fe distance. The Fe–Fe distances in **1–4** are 6.478, 5.677, 5.790, and 5.740 Å, respectively (figure 6). As the Fe–Fe distance in **4** is smaller than that of **1** and **3**, the ΔE of **4** should be larger than that of **1** and **3**. These results do not accord with the prediction (the ΔE of **4** is the smallest in figure 5). Hence, the direct Fe–Fe distance is not the only factor for ΔE of the carbon-bridged diferrocenyl derivatives.

Köhler *et al.* [20] have reported that the dihedral angle of the two Cp rings influence the potential separations of the ferrocenyl units. The dihedral angles of **1–4** (figure 6) are 79.4, 72.8, 84.3, and 83.3°, respectively. The dihedral angle of two Cp ring planes in **3** is 84.3°, the ΔE should be smallest among the compounds according to Köhler's

Table 2. Selected bond lengths (Å) of **1–4**.

1		2		3		4	
C(1)–C(2)	1.405(8)	C(1)–C(5)	1.421(3)	C(1)–C(2)	1.414(4)	C(1)–C(5)	1.405(5)
C(1)–C(5)	1.416(8)	C(1)–C(2)	1.425(3)	C(1)–C(5)	1.414(3)	C(1)–C(2)	1.415(5)
C(2)–C(3)	1.422(9)	C(2)–C(3)	1.417(3)	C(2)–C(3)	1.418(4)	C(2)–C(3)	1.426(5)
C(3)–C(4)	1.401(8)	C(3)–C(4)	1.416(3)	C(3)–C(4)	1.410(4)	C(3)–C(4)	1.406(5)
C(4)–C(5)	1.425(8)	C(4)–C(5)	1.427(3)	C(4)–C(5)	1.407(4)	C(4)–C(5)	1.425(4)
C(6)–C(7)	1.423(8)	C(6)–C(10)	1.426(3)	C(6)–C(7)	1.424(3)	C(6)–C(10)	1.428(4)
C(6)–C(10)	1.432(7)	C(6)–C(7)	1.430(3)	C(6)–C(10)	1.433(3)	C(6)–C(7)	1.429(4)
C(7)–C(8)	1.423(8)	C(7)–C(8)	1.419(3)	C(7)–C(8)	1.418(3)	C(7)–C(8)	1.416(4)
C(8)–C(9)	1.419(7)	C(8)–C(9)	1.421(3)	C(8)–C(9)	1.431(3)	C(8)–C(9)	1.424(4)
C(9)–C(10)	1.441(8)	C(9)–C(10)	1.431(3)	C(9)–C(10)	1.427(3)	C(9)–C(10)	1.423(4)
C(10)–C(11)	1.526(7)	C(10)–C(11)	1.525(3)	C(10)–C(11)	1.519(3)	C(10)–C(11)	1.522(4)
C(11)–C(14)	1.524(8)	C(11)–C(12)	1.532(3)	C(11)–C(12)	1.528(3)	C(11)–C(12)	1.541(4)
C(11)–C(13)	1.533(7)	C(11)–C(13)	1.554(3)	C(11)–C(13)	1.555(3)	C(11)–C(18)	1.546(3)
C(11)–C(12)	1.546(7)	C(13)–C(14)	1.525(3)	C(13)–C(14)	1.525(3)	C(16)–C(17)	1.391(4)
C(14)–C(15)	1.418(8)	C(15)–C(19)	1.427(3)	C(14)–C(15)	1.525(3)	C(19)–C(20)	1.422(4)
C(14)–C(18)	1.431(8)	C(15)–C(16)	1.433(3)	C(16)–C(17)	1.428(3)	C(19)–C(23)	1.426(4)
C(15)–C(16)	1.423(8)	C(16)–C(17)	1.429(3)	C(16)–C(20)	1.436(3)	C(20)–C(21)	1.425(4)
C(16)–C(17)	1.413(9)	C(17)–C(18)	1.412(4)	C(17)–C(18)	1.429(3)	C(21)–C(22)	1.416(4)
C(17)–C(18)	1.416(8)	C(18)–C(19)	1.429(3)	C(18)–C(19)	1.417(3)	C(22)–C(23)	1.424(4)
C(19)–C(20)	1.405(8)	C(20)–C(24)	1.425(3)	C(19)–C(20)	1.426(3)	C(24)–C(28)	1.409(4)
C(19)–C(23)	1.431(8)	C(20)–C(21)	1.426(3)	C(21)–C(25)	1.416(3)	C(24)–C(25)	1.423(4)
C(20)–C(21)	1.419(8)	C(21)–C(22)	1.421(3)	C(21)–C(22)	1.416(4)	C(25)–C(26)	1.416(4)
C(21)–C(22)	1.429(8)	C(22)–C(23)	1.424(3)	C(22)–C(23)	1.421(3)	C(26)–C(27)	1.412(4)
C(22)–C(23)	1.431(8)	C(23)–C(24)	1.410(3)	C(23)–C(24)	1.420(3)	C(27)–C(28)	1.429(4)

prediction [20], but it is the largest one. Hence, the effect of dihedral angle of the two rings on the ΔE value is still unclear.

Comparing redox potentials of **1–4** (figure 5), redox potentials of **2** and **3** shift negatively, and the redox potential of **4** shifts positively compared to **1**. The phenyl is electron-withdrawing to the bridge carbon, while the ethyl and propyl are electron donors to the bridge carbon. We calculated the charge numbers of bridging carbon of compounds **1**, **2**, and **4** by using density functional theory (DFT). The basis set used in the calculations was 6-31G. The calculated Mulliken atomic charges of **1**, **2**, and **4** were -0.0978 , -0.0473 , and -0.1398 , respectively. The results indicated that the charge density of carbon was lowered by the electron-withdrawing effect of phenyl and was improved by the electron-donating effect of ethyl. Synchronously, the frontier orbital electronic structure of **1**, **3**, and **4** was also investigated by computation methods based on a starting geometry from the X-ray structure analysis (figure 7); calculations were carried out using the B3LYP functional and the 6-31G basis set for geometric optimization [21]. As expected, the HOMO, LUMO, and HOMO-1 of **1** and **3** are mainly localized on the ferrocenyl units, but the HOMO and HOMO-1 of **4** is mainly localized on the phenyl unit and the LUMO of **4** is localized on one ferrocenyl unit. This is in good agreement with the cyclic voltammetric data. The HOMO of **4** localized on phenyl is ascribed to the electron withdrawing effect of phenyl, which makes the ferrocenyl oxidation difficult, so the first oxidation potential of **4** shifts positively. The electron density of HOMO-1 of **4** still partially localizes on the phenyl, which indicates that even one oxidized ferrocenyl in the phenyl has a stronger electron-withdrawing capability to reduce the

Table 3. Selected bond angles (°) of 1–4.

1	2	3	4
C(2)–C(1)–C(5)	C(5)–C(1)–C(2)	C(2)–C(1)–C(5)	C(5)–C(1)–C(2)
C(1)–C(2)–C(3)	C(3)–C(2)–C(1)	C(1)–C(2)–C(3)	C(1)–C(2)–C(3)
C(4)–C(3)–C(2)	C(4)–C(3)–C(2)	C(4)–C(3)–C(2)	C(4)–C(3)–C(2)
C(3)–C(4)–C(5)	C(3)–C(4)–C(5)	C(5)–C(4)–C(3)	C(3)–C(4)–C(5)
C(1)–C(5)–C(4)	C(1)–C(5)–C(4)	C(1)–C(5)–C(1)	C(1)–C(5)–C(4)
C(7)–C(6)–C(10)	C(10)–C(6)–C(7)	C(7)–C(6)–C(10)	C(10)–C(6)–C(7)
C(8)–C(7)–C(6)	C(8)–C(7)–C(6)	C(8)–C(7)–C(6)	C(8)–C(7)–C(6)
C(9)–C(8)–C(7)	C(7)–C(8)–C(9)	C(7)–C(8)–C(9)	C(7)–C(8)–C(9)
C(8)–C(9)–C(10)	C(8)–C(9)–C(10)	C(10)–C(9)–C(8)	C(10)–C(9)–C(8)
C(6)–C(10)–C(9)	C(6)–C(10)–C(9)	C(9)–C(10)–C(6)	C(9)–C(10)–C(6)
C(6)–C(10)–C(11)	C(6)–C(10)–C(11)	C(9)–C(10)–C(11)	C(10)–C(11)–C(19)
C(9)–C(10)–C(11)	C(9)–C(10)–C(11)	C(6)–C(10)–C(11)	C(10)–C(11)–C(12)
C(10)–C(11)–C(14)	C(10)–C(11)–C(15)	C(10)–C(11)–C(16)	C(10)–C(11)–C(18)
C(14)–C(11)–C(13)	C(10)–C(11)–C(12)	C(10)–C(11)–C(12)	C(10)–C(11)–C(18)
C(14)–C(11)–C(13)	C(15)–C(11)–C(12)	C(16)–C(11)–C(12)	C(19)–C(11)–C(18)
C(10)–C(11)–C(12)	C(10)–C(11)–C(13)	C(10)–C(11)–C(13)	C(12)–C(11)–C(18)
C(13)–C(11)–C(12)	C(12)–C(11)–C(13)	C(12)–C(11)–C(13)	C(17)–C(12)–C(11)
C(15)–C(14)–C(11)	C(14)–C(13)–C(11)	C(14)–C(13)–C(11)	C(13)–C(12)–C(11)
C(18)–C(14)–C(11)	C(19)–C(15)–C(16)	C(15)–C(14)–C(13)	C(14)–C(13)–C(12)
C(14)–C(15)–C(16)	C(16)–C(15)–C(11)	C(17)–C(16)–C(20)	C(16)–C(15)–C(14)
C(17)–C(16)–C(15)	C(16)–C(15)–C(11)	C(17)–C(16)–C(11)	C(15)–C(16)–C(17)
C(16)–C(17)–C(18)	C(18)–C(17)–C(16)	C(16)–C(17)–C(18)	C(20)–C(19)–C(23)
C(17)–C(18)–C(14)	C(17)–C(18)–C(19)	C(19)–C(18)–C(17)	C(23)–C(19)–C(11)
C(20)–C(19)–C(23)	C(15)–C(19)–C(18)	C(18)–C(19)–C(20)	C(19)–C(20)–C(21)
C(19)–C(20)–C(21)	C(24)–C(20)–C(21)	C(25)–C(21)–C(22)	C(21)–C(22)–C(23)
C(20)–C(21)–C(22)	C(21)–C(22)–C(23)	C(24)–C(23)–C(25)	C(28)–C(24)–C(25)
C(21)–C(22)–C(23)	C(24)–C(23)–C(22)	C(25)–C(24)–C(23)	C(26)–C(25)–C(24)
C(22)–C(23)–C(19)	C(23)–C(24)–C(20)	C(21)–C(25)–C(24)	C(26)–C(27)–C(28)
108.7(6)	108.14(18)	108.14(18)	108.0(2)
108.0(6)	107.90(18)	107.90(18)	107.7(2)
107.7(6)	108.20(18)	108.20(18)	107.9(2)
108.7(6)	108.19(18)	108.19(18)	108.3(2)
106.9(5)	107.57(18)	107.57(18)	108.0(2)
108.4(5)	108.64(16)	108.64(16)	108.78(19)
108.6(5)	107.78(17)	107.78(17)	107.86(19)
107.5(5)	107.97(17)	107.97(17)	107.99(19)
109.1(5)	108.79(17)	108.79(17)	108.51(19)
106.5(5)	106.83(16)	106.83(16)	106.86(18)
125.7(5)	127.04(16)	127.04(16)	126.75(18)
127.5(5)	125.75(16)	125.75(16)	126.26(18)
106.6(5)	109.05(14)	109.05(14)	108.29(16)
110.5(5)	110.83(15)	110.83(15)	110.35(17)
111.6(5)	110.44(15)	110.44(15)	111.06(17)
110.6(4)	107.55(14)	107.55(14)	108.55(16)
109.9(5)	108.67(15)	108.67(15)	108.46(17)
107.7(5)	110.23(15)	110.23(15)	110.06(17)
106.4(6)	115.59(16)	115.59(16)	117.85(18)
126.7(6)	107.03(18)	107.03(18)	110.54(19)
126.6(6)	126.30(18)	126.30(18)	106.89(18)
109.2(6)	126.50(19)	126.50(19)	126.16(19)
107.4(7)	108.5(2)	108.5(2)	126.63(19)
108.2(6)	107.84(19)	107.84(19)	108.73(19)
108.7(6)	108.3(2)	108.3(2)	107.77(19)
108.5(6)	108.3(2)	108.3(2)	108.32(19)
108.4(6)	107.4(2)	107.4(2)	108.1(2)
108.0(5)	107.5(2)	107.5(2)	108.1(2)
107.6(6)	108.45(19)	108.45(19)	107.7(2)
107.4(6)	108.34(19)	108.34(19)	108.2(2)

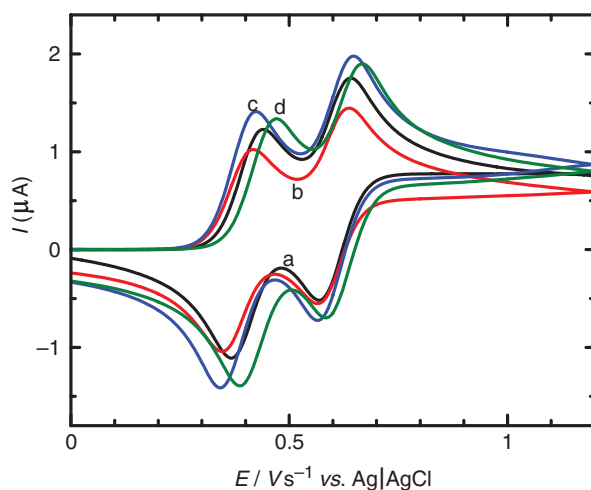


Figure 5. Cyclic voltammograms of (a) **1** (black line), (b) **2** (red line), (c) **3** (blue line) and (d) **4** (green line).

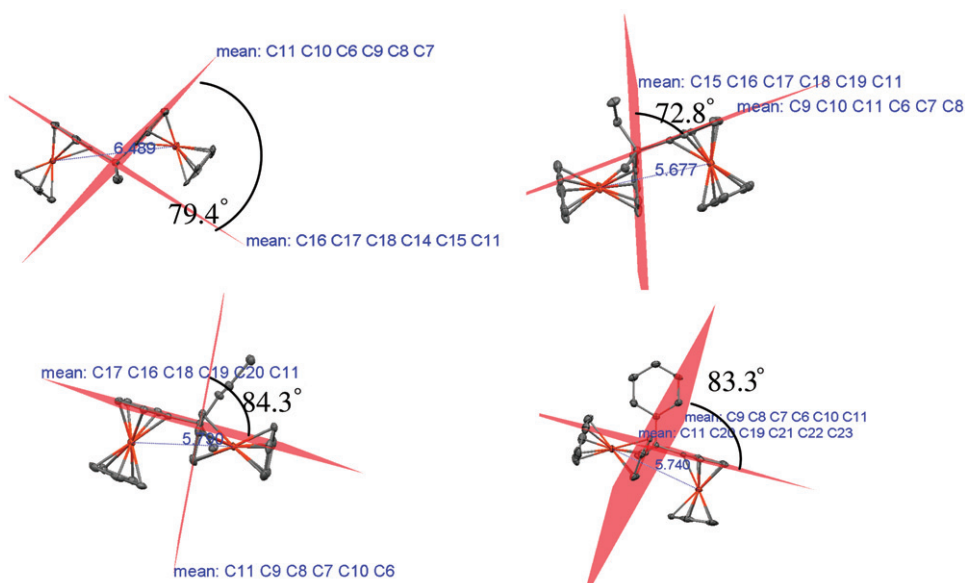


Figure 6. Dihedral angles of Cp-ring plane of two ferrocenyl and Fe-Fe distance of **1-4**.

charge density of bridge “C”. Thus, the ΔE value of **4** is smallest. The redox potential and potential separation of **1-4** exhibit different characters due to the change of the charge density of the bridging carbon, ΔE decreased with the decreasing charge density of the bridge “C”. Therefore, the charge density of the bridging carbon was the key factor for electrochemical interactions between ferrocenyl units of diferrocenyl derivatives.

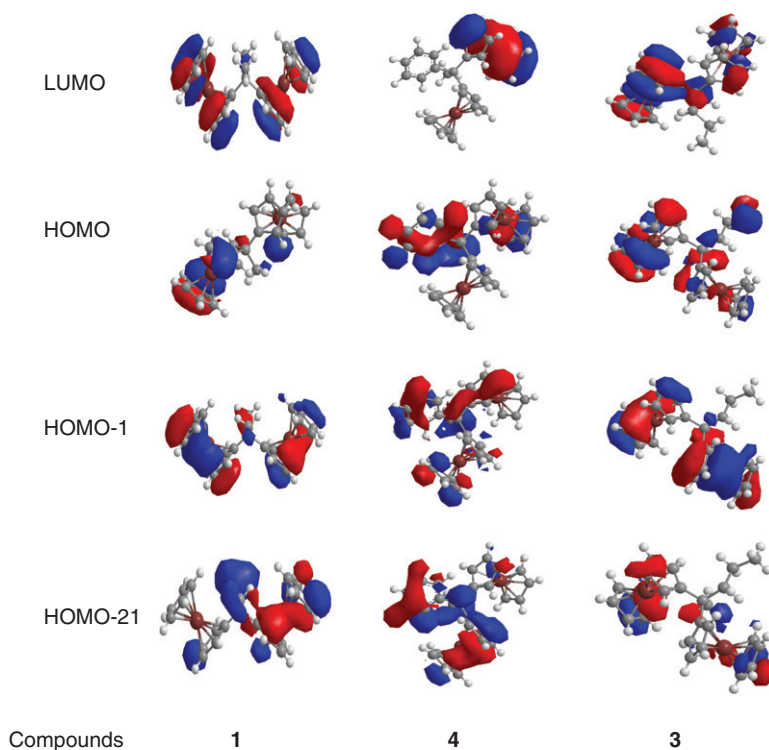


Figure 7. DFT computed frontier orbitals of **1**, **2**, and **4**.

4. Conclusion

Four diferrocenyl compounds: $\text{FcC}(\text{CH}_3)_2\text{Fc}$, $\text{Fc}(\text{CH}_3)\text{C}(\text{C}_2\text{H}_5)\text{Fc}$, $\text{Fc}(\text{CH}_3)\text{C}(\text{C}_3\text{H}_7)\text{Fc}$, and $\text{Fc}(\text{CH}_3)\text{C}(\text{C}_6\text{H}_5)\text{Fc}$ were synthesized by the acid-catalyzed condensation of ferrocene and corresponding ketone. The molecular structures were determined by using NMR, FT-IR, MS, elemental analysis, and X-ray single crystal diffraction. Electrochemical interactions between ferrocenyl units in these compounds were investigated by cyclic voltammetry, molecular structure analysis, and calculation. By comparing the charge density based on calculation, we found that the electronic property of the bridging carbon was the pivotal factor for the potential separation of two ferrocenyl units in **1–4**.

Supplementary material

Crystallographic data for the structural analysis have been deposited at the Cambridge Crystallographic Data Centre, CCDC No. 752522, 752523, 752524, and 752525 for **1**, **2**, **3**, and **4**, respectively. Copies of this information may be obtained free of charge from the Director, CCDC, 12 Union Road, Cambridge CB2 1EZ, UK (Fax: +44-1223-336033; Email: deposit@ccdc.cam.ac.uk).

Acknowledgments

We are grateful to the Specialized Research Fund for the Doctoral Program of Higher Education of China (20060128001), the Program for New Century Excellent Talents in University (NCET-08-858), and the Natural Science Foundation of the Inner Mongolia (20070128001) and (20080404MS020).

References

- [1] C. Engtrakul, L.R. Sita. *Nano Lett.*, **1**, 541 (2001).
- [2] W.H. Morrison, S. Krogsrud, D.N. Hendrickson. *Inorg. Chem.*, **12**, 1998 (1973).
- [3] V.V. Dementev, F. Cervanteslee, L. Parkanyi, H. Sharma, K.H. Pannell, M.T. Nguyen, A. Dlaz. *Organometallics*, **12**, 1983 (1993).
- [4] G.M. Brown, T.J. Meyer, D.O. Cowan, C.L. Vanda, F. Kaufman, P.V. Roling, M.D. Rausch. *Inorg. Chem.*, **14**, 506 (1975).
- [5] P. Shu, K. Bechgaard, D. Cowan. *J. Org. Chem.*, **41**, 1849 (1976).
- [6] J.E. Gorton, H.L. Lentzner, W.E. Watts. *Tetrahedron*, **27**, 4353 (1971).
- [7] R. Rulkens, A.J. Lough, I. Manners. *J. Am. Chem. Soc.*, **116**, 797 (1994).
- [8] J.C. Kotz, C.L. Nivert, J.M. Lieber, R.C. Reed. *J. Organomet. Chem.*, **91**, 87 (1975).
- [9] P. Zanello, G. Opromolla, M. Herberhold, H.D. Brendel. *J. Organomet. Chem.*, **484**, 67 (1994).
- [10] C. Levanda, K. Bechgaard, D.O. Cowan. *J. Org. Chem.*, **41**, 2700 (1976).
- [11] M.R. Burgess, S. Jing, C.P. Morley. *J. Organomet. Chem.*, **691**, 3484 (2006).
- [12] Y. Matsuura, K. Matsukawa. *Chem. Phys. Lett.*, **428**, 321 (2006).
- [13] Z.H. Weng, Z.L. Chen, F.P. Liang. *J. Coord. Chem.*, **62**, 1801 (2009).
- [14] X. Li, B.L. Wu, W. Liu, C.Y. Niu, Y.Y. Niu, H.Y. Zhang. *J. Coord. Chem.*, **62**, 3142 (2009).
- [15] C.J. Qiao, J. Li, Y. Xu, S.Y. Guo, X. Qi, Y.T. Fan. *J. Coord. Chem.*, **62**, 3268 (2009).
- [16] R. Rulkens, A.J. Lough, I. Manners, S.R. Lovelace, C. Grant, W.E. Geiger. *J. Am. Chem. Soc.*, **118**, 12683 (1996).
- [17] C. Patoux, C. Coudret, J.P. Launay, C. Joachim, A. Gourdon. *Inorg. Chem.*, **6**, 5037 (1997).
- [18] W.Y. Liu, Y.F. Yuan, L.Y. Zhang. *J. Chinese Univ.*, **19**, 1251 (1998).
- [19] Bruker. *SHELXTL*, Bruker Analytical X-ray Instruments Inc., Madison, WI (1997).
- [20] H. Atzkern, F.H. Köhler, R.Z. Müller. *Naturforschung*, **45B**, 329 (1990).
- [21] V.O. Nyamori, S.D. Mhlanga, N.J. Coville. *J. Organomet. Chem.*, **693**, 2205 (2008).